



HHS Public Access

Author manuscript

Mol Psychiatry. Author manuscript; available in PMC 2012 November 01.

Published in final edited form as:

Mol Psychiatry. 2012 May ; 17(5): 471–558. doi:10.1038/mp.2011.81.

Aging and Functional Brain Networks

Dardo Tomasi, Ph.D.^{*1} and Nora D. Volkow, M.D.^{1,2}

¹ National Institute on Alcohol Abuse and Alcoholism, Bethesda, MD, 20892

² National Institute on Drug Abuse, Bethesda, MD, 20892

Abstract

Aging is associated with changes in human brain anatomy and function and cognitive decline. Recent studies suggest the aging decline of major functional connectivity hubs in the “default-mode” network (DMN). Aging effects on other networks, however, are largely unknown. We hypothesized that aging would be associated with a decline of short- and long-range functional connectivity density (FCD) hubs in the DMN. To test this hypothesis we evaluated resting-state datasets corresponding to 913 healthy subjects from a public magnetic resonance imaging database using *functional connectivity density mapping*, a voxelwise and data-driven approach together with parallel computing. Aging was associated with pronounced long-range FCD decreases in DMN and dorsal attention network (DAN) and with increases in somatosensory and subcortical networks. Aging effects in these networks were stronger for long-range than for short-range FCD and were also detected at the level of the main functional hubs. Females had higher short- and long-range FCD in DMN and lower FCD in the somatosensory network than males, but the gender by age interaction effects were not significant for any of the networks or hubs. These findings suggest that long-range connections may be more vulnerable to aging effects than short-range connections and that in addition to the DMN the DAN is also sensitive to aging effects, which could underlie the deterioration of attention processes that occurs with aging.

Keywords

Aging; Connectivity; Alzheimer’s disease; Functional Connectomes

INTRODUCTION

As we age the brain experiences anatomical and functional changes and cognitive decline^{1,2}. Aging is associated with functional disruption of cortical networks involving precuneus, retrosplenial and posterior cingulate cortices³, hypo activation of prefrontal networks and compensatory cortical recruitment^{4,5}. In elderly Alzheimer’s disease (AD) patients, deposition of amyloid plaques in precuneus, retrosplenial and posterior cingulate cortices has been linked to atrophy and lower metabolic rate of glucose in these brain regions in

Users may view, print, copy, download and text and data- mine the content in such documents, for the purposes of academic research, subject always to the full Conditions of use: http://www.nature.com/authors/editorial_policies/license.html#terms

Corresponding author: Dardo Tomasi (tomasi@bnl.gov), Ph.D., Laboratory of Neuroimaging (LNI/NIAAA), Medical Department, Bldg 490, Brookhaven National Laboratory, 30 Bell Ave., Upton, NY, 11973, USA, Phone: (631) 344-5577 Fax: (631) 344-5576.

association with accelerated cognitive decline^{6,7}. Magnetic resonance imaging (MRI) studies in “resting-state” conditions have identified the same regions that show high amyloid deposition in AD patients with the major functional brain hubs (regions with high functional connectivity density)⁸. Amyloid deposition in precuneus, retrosplenial and posterior cingulate cortices has also been shown in older adults^{9,10} but the potential effects of normal aging on functional hubs have not been investigated. Thus we aimed to evaluate aging effects on functional connectivity hubs in a large sample of healthy subjects.

The functional connectivity among brain regions can be estimated from spontaneous fluctuations of brain activity captured during brief MRI scanning (5-min) in resting conditions (10) and used to study age-related changes in the brain¹¹. Functional hubs can be evaluated from these “resting-state” (RS-fMRI) datasets using computer-demanding data-driven approaches based on graph theory^{8,12,13}, which were shown to correspond well with structural connections determined with diffusion tensor imaging¹⁴ and to be associated with intellectual performance¹⁵. Recently, we proposed *functional connectivity density mapping* (FCDM)¹⁶, an ultra-fast voxelwise data-driven method to measure *local* FCD hubs in humans, and showed that the most prominent *short-range* FCD hubs are functionally connected to cortical and subcortical networks¹⁷. However, the main limitation of FCDM was that it does not account for *long-range* hubs¹⁸. Here we complement FCDM with computationally demanding graph theory measures of *global* FCD to detect *long-range* FCD hubs.

The present study assesses the effect of normal aging on short- and long-range FCD hubs in 913 subjects from a large public MRI database¹⁹. We used FCDM and parallel computing to speed up the calculation of short- and long-range FCD maps with 3-mm isotropic resolution. Multi-regression statistical parametric mapping and complementary non-parametric tests were used to identify brain regions exhibiting aging and gender effects on short- and long-range FCD. We hypothesized that the decline of the functional hubs with age would vary across brain networks. Specifically, we hypothesized that the strength of the hubs in the default-mode network (DMN: retrosplenial cortex, posterior cingulate and ventral prefrontal cortices, precuneus and angular gyrus) would decrease with age⁹ more prominently for long-range than for short-range hubs and, more exploratory, that the strength of the hubs in other networks would show concomitant age-related increases in FCD, paralleling those documented by fMRI studies^{4,5}.

METHODS

Subjects

Functional scans that were collected in resting conditions and correspond to 913 healthy subjects (Supp Table 1) from 19 research sites of the “1000 Functional Connectomes” Project (http://www.nitrc.org/projects/fcon_1000/) were included in the study. Datasets from other research sites that were not available at the time of the study (pending verification of IRB status), did not report demographic variables (gender and age), exhibited image artifacts that prevented the study of short- and long-range FCD, or did not meet the imaging acquisition criteria (3s TR, full brain coverage, time points > 100, spatial resolution better than 4-mm) were not included in the study.

Image preprocessing

Image realignment and spatial normalization to the stereotactic space of the Montreal Neurological Institute (MNI) were carried out using the statistical parametric mapping package SPM2 (Wellcome Trust Centre for Neuroimaging, London, UK). A 4th degree B-spline function without weighting and without warping was used for image realignment, and a 12-parameters affine transformation with medium regularization, 16-nonlinear iterations, voxel size of $3 \times 3 \times 3 \text{ mm}^3$ was used for spatial normalization. Other preprocessing steps were carried out using IDL (ITT Visual Information Solutions, Boulder, CO). Motion-related fluctuations were removed from the MRI signals using multilinear regression with the six time-varying realignment parameters (3 translations and 3 rotations)¹⁶. Global signal intensity was normalized across time points. Band-pass temporal filtering (0.01–0.10 Hz) was used to remove magnetic field drifts of the scanner²⁰ and minimize physiologic noise of high frequency components²¹. Voxels with signal-to-noise (as a function of time) < 50 were eliminated to minimize unwanted effects from susceptibility-related signal-loss artifacts on FCDM. MRI time series reflecting the preprocessing steps were saved in hard drive for subsequent analyses.

Global FCD

Pearson linear correlation was used to map the strength of the *global functional connectivity density* (gFCD) from individual preprocessed time series²². Two voxels with correlation factor $R > 0.6$ were considered functionally connected; this arbitrary correlation threshold was selected to be consistent with the threshold used for the calculation of the *IFCD*¹⁶. The gFCD at a given voxel x_0 was computed as the *global* number of functional connections, $k(x_0)$, between x_0 and all other $N = 57,713$ voxels in the brain. This calculation was repeated for all x_0 voxels in the brain involving the computation of a correlation matrix with N^2 elements. A parallel algorithm that takes advantage of multiprocessor computer architectures was developed in C-language to speed up the calculation of the gFCD. A workstation with two Intel® Xeon® X5680 processors (12MB L3 Cache, 64-bit, 3.33 GHz) running Windows 7 was used to compute the gFCD maps for each subject. In average, the parallel gFCD-algorithm required only five minutes/subject to complete when all 24 processing threads were available.

Local FCD

The preprocessed image time series underwent FCDM¹⁶ to compute the strength of the *IFCD*. Specifically, we computed Pearson correlations between time-varying signals at x_0 and those at its local neighbors. A voxel (x_j) was added to the list of neighbors of x_0 (x_N ; $N = \{i\}$) only if it was adjacent to a voxel that was linked to x_0 by a continuous path of functionally connected voxels and $R_{0j} > 0.6$. This calculation was repeated for all voxels that were adjacent to voxels that belonged to the list of neighbors of x_0 in an iterative manner until no new neighbors could be added to the list. The *IFCD* of x_0 was computed as the number of elements in the local functional connectivity cluster, $k(x_0)$. Then the calculation was initiated for a different x_0 . This “growing” algorithm was developed in IDL¹⁶. Whereas this calculation is performed for all N voxels in the brain the necessary correlations to compute a map of the *IFCD* is reduced by a large factor (~ 1000).

Short- and long-range FCD

The *l*FCD included all voxels that belonged to the local cluster of functionally connected voxels and was equated to *short-range* FCD. The strength of the *long-range* FCD was equated to *g*FCD – *l*FCD in order to isolate distal connections. Short- and long-range FCD maps were spatially smoothed (8-mm) in SPM to minimize the differences in the functional anatomy of the brain across subjects, and normalized to their average strength in the whole brain in order to minimize variability across research sites.

Statistical analyses

A multiple regression approach with two zero-mean regressors (age and gender) was implemented in SPM to map the aging effects on short- and long-range FCD. Short- and long-range FCD maps from all 913 subjects were included in the analysis. Statistical results were corrected for multiple comparisons using the continuous random field calculation implemented in SPM2²³. A conservative family-wise error (FWE) threshold $P_{corr} < 0.05$, corrected for multiple comparisons at the voxel-level, was used to display statistical maps reflecting correlations between FCD and age.

Region-of-interest (ROI) analyses

Isotropic cubic masks containing 27 imaging voxels (0.73 ml) were defined at the coordinates of the cluster centers in the right hemisphere (Table 1) to extract the average strength of the short- and long-range FCD from individual maps and using a custom program written in IDL. The coordinates of the masks were kept fixed across subjects. The ROI measures were used to assess the significance of the findings (assessed with parametric Pearson and non-parametric Spearman correlations) in a cluster of voxels rather than in single voxels. Statview (SAS Institute Inc, Cary, NC) was used for this purpose.

RESULTS

Short- and long-range functional connectivity

The average distribution of the short-range FCD was maximal in posterior cingulate/ventral precuneus (PC/VP). Inferior, superior and lateral (angular gyrus) parietal, occipital, somatosensory and ventral and dorsolateral prefrontal (DLPFC) cortices also included prominent short-range FCD hubs (Fig 1A). Short-range FCD hubs in subcortical regions were weaker than those in cortical regions. The average distribution of the long-range FCD was maximal in the occipital cortex (Fig 1A and Table 1). PC/VP, angular gyrus, superior and inferior parietal, DLPFC and temporal cortices also had significant long-range FCD. Note that the patterns of these highly connected regions (both short- and long-range) had a bilateral distribution in the brain. We evaluated the strength of short- and long-range hubs in 7 networks that were previously identified from the most prominent 4 cortical and 3 subcortical FCD hubs¹⁷. Using parametric (Pearson) and non-parametric (Spearman) correlations, we verified that the average strength of the short-range FCD was correlated with that of the long-range FCD in all networks ($P < 0.0001$; Fig 1B). Whereas the linear association was rather constant across networks (regression slope = 0.21 ± 0.01 ; mean \pm SE)

the excursions of short- and long-range FCD across subjects were larger for the visual network and DMN than for the remaining five networks.

Aging

The long-range FCD in default mode network (DMN; posterior cingulate, precuneus, angular gyrus and ventral prefrontal cortex) and in middle orbitofrontal and middle and dorsolateral prefrontal cortices decreased with age, and that in somatosensory and motor cortex, insula, caudate, hippocampus, thalamus, cerebellum and brainstem increased with age ($P_{corr} < 0.0001$, Fig 2A and Table 1). Aging effects on short-range FCD overlapped but were much more localized and weaker than for long-range FCD and additionally involved age-related decreases in ventral striatum (Fig 2B and Table 1).

The analysis of average FCD measures in seven different networks¹⁷ revealed prominent age-related FCD-decreases in DMN and dorsal attention network (DAN) and FCD-increases in the somatosensory and cerebellar networks on both short- and long-range connections ($P < 10^{-5}$; Fig 3A). Age-related FCD-increases in the other two subcortical networks (thalamus and amygdala) were significant for long-range connections ($P < 10^{-5}$) but not for the short-range connections (Supp Fig 1).

The ROI analysis of FCD measures at the location of main cortical (PC/VP, inferior parietal, cuneus and somatosensory cortices) and subcortical (cerebellum, thalamus, and amygdala) hubs revealed pronounced age-related decreases in long-range FCD in PC/VP (BA 23/31), which is the core of the DMN¹⁷ and the strongest local FCD hub in the brain¹⁶, and increases in short- and long-range FCD in postcentral gyrus (BA 3), which is the core hub of the somatosensory network¹⁷, and in thalamus ($P < 10^{-5}$; Fig 3B).

Gender effects

The voxelwise analysis revealed strong gender effects for long- and for short-range FCD. Specifically, long-range FCD was higher in DMN regions (posterior cingulate, ventral precuneus, angular gyrus, and ventral prefrontal cortex), parahippocampal gyrus, amygdala and thalamus and it was lower in somatosensory and motor cortex for females than for males ($P_{corr} < 0.0005$). The VOI analysis to assess gender effects in the seven major networks demonstrated that short- and long-range connections were stronger in the DMN and weaker in the somatosensory network for females than for males ($P < 0.003$; Fig 4A). The short-range FCD in the amygdala network was higher for males than for females ($P < 0.001$). The ROI analysis assessing gender effects in the major cortical and subcortical hubs showed that short- and long-range connections in PostCG (main hub of the somatosensory network) were weaker for females than for males ($P < 0.005$; Fig 4B), whereas short-range FCD in amygdala (main hub of amygdala network) and long-range FCD in PC/VP (main hub of DMN), were higher for females than for males ($P < 0.002$). Differential gender effects in short-range FCD for the amygdala hub and the amygdala network might reflect the strength of the PostCG hub (two times stronger than the amygdala hub) and the extensive overlap between the somatosensory network and the amygdala network¹⁷. Gender \times age interaction effects were not statistically significant for any of the seven networks and for any of the seven hubs ($P > 0.3$).

DISCUSSION

Growing evidence suggests that human cognitive capacity suffers continuous decline during the lifespan, starting in early adulthood. This decline is likely to reflect age-related changes in brain neurotransmission and structure, which are not uniform (frontal and temporal cortices being among the most affected)²⁴. The aging decline of neurotransmitter systems selectively impairs regional brain function (i.e. decreases in dopamine neurotransmission are linked to decline in frontal function)^{25,26} and the deterioration of the axonal myelin sheath with age degrades the long-range connectivity of specific neural networks (reviewed by Madden²⁷). However there is also evidence that some networks might be preserved and it is speculated that these may help to compensate for age effects in brain function^{28,29}. Similarly age related decreases in cognitive performance are not uniform, attention, memory and executive function (including working memory) are the most affected³⁰ whereas some cognitive functions are relatively preserved (language, decision making)^{31,32}. Thus a better characterization of the effects of aging on brain functional networks is of value to help understand better the unique pattern of cognitive decline associated with aging and potential mechanisms for compensation.

Here we document aging and gender effects on short- and long-range FCD in 913 healthy subjects from the image repository “1000 Functional Connectomes” using a data-driven approach at 3-mm isotropic resolution. In addition to the previously described age-associated decreases in connectivity of DMN we also showed FCD-decreases in DAN regions as well as FCD-increases in somatosensory and motor cortex, amygdala and thalamus. Overall aging effects were more pronounced for long-range FCD than for short-range FCD. We also document significant gender differences in network and hub connectivity but showed no significant age by gender interaction effects on long- or short-range FCD.

The main hubs of long- and short-range connectivity were located in posterior ventral parietal/posterior cingulate (main short-range hub and prominent long-range hub) and occipital cortices (main long-range hub). This finding is consistent with previous MRI studies based on graph theory that reported that PC/VP and occipital cortices house prominent hubs of global^{8,12} and local¹⁶ functional connectivity, as well as with PET studies showing high metabolic rate of glucose in these posterior brain regions^{33,34}. The PC/VP hub is interconnected with all DMN regions¹⁷ that show synchronous signal fluctuations and high metabolism in resting conditions, and negative fMRI responses during cognition^{17,35,36}. The occipital cortex has the highest neuronal density among cortical regions³⁷ and is essential for visual processing³⁸. Recently we have shown that the occipital FCD hubs are highly interconnected with an occipital-parietal network that shows overlap with the posterior dorsal attention network¹⁷.

In average, the strength of long-range FCD hubs in the DMN decreased $6 \pm 1\%$ per decade of life and that of short-range connectivity $1.6 \pm 0.3\%$ per decade of life. The decreases were even more pronounced at the location of PC/VP (long-range FCD: $12 \pm 2\%$ per decade of life; short-range FCD: $4 \pm 2\%$ per decade of life). The sensitivity of the DMN to aging effects is consistent with reduced resting-state activity³⁹ and disruption of cortical networks

caused by amyloid deposition⁹ and potential gliosis⁴⁰ in precuneus, retrosplenial and posterior cingulate cortices in older adults, and suggest that resting-state MRI acquisition could serve as a biomarker of aging in the human brain⁴¹. Moreover, decreases in DMN connectivity with aging have been associated with impaired performance in working memory⁴². However, the aging effects on long-range FCD hubs in the posterior cingulate differ from those on glucose metabolism, which have noted relative resilience of this brain region to the effects of aging and have contrasted this with the higher sensitivity of metabolic decreases in AD⁴³.

FCD-decreases with age were also observed in DAN (long-range: $3.4 \pm 0.8\%$ per decade of life; short-range: $1.7 \pm 0.3\%$ per decade of life) that includes prefrontal cortex, anterior cingulate (ACC) and posterior parietal cortices. This finding is consistent with the age-related decline in glucose metabolism documented by positron emission tomography studies, which shows that the most prominent decreases in metabolic activity in the healthy brain occur in prefrontal cortex (PFC) and in ACC^{25,43,44}. Decreases in FCD in the DAN could underlie the impairments in sustained attention, which is one of the most affected cognitive functions that occurs with aging⁴⁵. In healthy individuals we have shown that the age related decline in striatal dopamine D2 receptors is associated with age-related attention deficits, which in turn are associated with decreased activity in PFC and ACC⁴⁶. Moreover, in healthy controls the dopamine enhancing drug methylphenidate increased activation of the DAN while it increased deactivation of the DMN during performance of a visual attention task⁴⁷ suggesting that the age related decline in dopamine neurotransmission may contribute to the decreased FCD in DAN,

Conversely, there were concomitant age-related increases in long-range FCD in other networks (somatosensory: $6 \pm 1\%$ per decade of life; cerebellum, thalamus, and amygdala: $20 \pm 3\%$ per decade of life) that are consistent with increases in brain activation^{4,5,48} and functional connectivity¹⁹ in prefrontal regions for older compared to younger individuals. These results conform well with findings from studies investigating the effects of normal aging on brain glucose metabolism most of which have shown that in addition to the posterior cingulate, the thalamus, cerebellum, striatum and limbic structures (including amygdala) are the least affected by aging (reviewed by Kalpouzos⁴³). Moreover a longitudinal study reported significant increases in regional cerebral blood flow with age in cerebellum, thalamus and putamen in addition to the significant decreases in prefrontal regions⁴⁹.

To our knowledge there are no prior reports that differentially evaluate the aging effect on short vs. long-range functional connectivity. The higher sensitivity of the long-range FCD, compared to that of the short-range FCD, suggests that long-range connections may be more vulnerable to aging effects than short-range connections. The physiological significance of this is unclear but we speculate that longer fibers may be more vulnerable to degeneration than shorter ones since proteins have to travel longer distances and hence are more vulnerable to energy deficits. While there is no current evidence in the human brain in peripheral neurons the length of the axons has been associated with their vulnerability to degenerative processes as is the case for amyotrophic lateral sclerosis and spastic paraplegias⁵⁰. Also aging has been associated, at least for the case of cholinergic fibers, with

a decrease in fiber length⁵¹. Similarly, postmortem studies have reported decreases in myelinated fiber length with age in the human brain⁵² (10% decrease per decade), which is likely to contribute to decreased long-range FCD with aging. However, a limitation on our interpretation for the greater vulnerability of long FCD to aging is the fact that long distance functional connectivity also relies on polysynaptic circuits, which may not necessarily entail longer fibers and since we did not have measures of fiber length (as per diffusion tensor imaging) we can not exclude this as a confound.

In this study we also find significant gender differences in FCD. Specifically short- and long-range FCD hubs were stronger in DMN and weaker in somatosensory network for females than for males. This is consistent with previous studies that documented gender effects in functional and anatomical connectivity^{19,53}. Higher long-range FCD in DMN in females than males is also in agreement with reports of higher cerebral blood flow and higher baseline glucose metabolism in DMN for females than for males^{54,55} and could help explain why female AD-patients show greater cognitive impairments than male patients for the equivalent reductions in regional brain metabolism⁵⁶. However in this study we failed to find significant gender by age interactions suggesting that aging effects on FCD may be similar for males and females.

Limitations

The 1000 functional connectomes database includes limited phenotypic characterization of the individuals. Thus it was not possible to ascertain the functional significance of the aging effects on short- or long-range FCD. More specifically, we were unable to evaluate confounds such as vascular risk, hormonal changes, genetic factors and cognitive aptitude that may be related to network properties. Since vascular risk increases with age we speculate that this could contribute to the age-related changes in long-range FCD and that the later in turn may underlie some of the changes in cognitive performance that occur with aging. However studies are needed to demonstrate this. Nonetheless the consistency of the findings from resting FCD patterns¹⁶ makes it possible to generate standards that can be used in subsequent studies to compare with patient populations. The cross-sectional study design made possible evaluation of aging effects during the lifespan but limits the interpretability of the results. Note that the accelerated evolution of medical imaging technology poses challenges for longitudinal studies of brain function during the lifespan to ensure that the data is comparable as spatial and temporal resolution of the imaging tools change.

Summary

We evaluated aging and gender effects on short- and long-range FCD in 913 healthy subjects. DMN and DAN exhibited age-related decreases that were more pronounced for long-range FCD than for short-range FCD. Age-related increases in FCD were found in somatosensory cortex (in females), limbic regions and thalamus.

Supplementary Material

Refer to Web version on PubMed Central for supplementary material.

Acknowledgments

Support: National Institutes of Alcohol Abuse and Alcoholism (2RO1AA09481).

References

1. Raz N. Differential aging of the brain: Patterns, cognitive correlates and modifiers. *Neurosci Biobehav Rev* Rodrigue, KM. 30:730–748.
2. Bäckman L, Nyberg L, Lindenberger U, Li S, Farde L. The correlative triad among aging, dopamine, and cognition: current status and future prospects. *Neurosci Biobehav Rev*. 2006; 30:791–807. [PubMed: 16901542]
3. Buckner R. Memory and Executive Function in Aging and AD: Multiple Factors that Cause Decline and Reserve Factors that Compensate. *Neuron*. 2004; 44:195–208. [PubMed: 15450170]
4. Logan J, Sanders A, Snyder A, Morris J, Buckner R. Under-recruitment and nonselective recruitment: dissociable neural mechanisms associated with aging. *Neuron*. 2002; 33:827–840. [PubMed: 11879658]
5. Davis S, Dennis N, Daselaar S, Fleck M, Cabeza R. Que PASA? The posterior-anterior shift in aging. *Cereb Cortex*. 2008; 18:1201–1209. [PubMed: 17925295]
6. Buckner R, Snyder A, Shannon B, LaRossa G, Sachs R, Fotenos A, et al. Molecular, structural, and functional characterization of Alzheimer's disease: evidence for a relationship between default activity, amyloid, and memory. *J Neurosci*. 2005; 25:7709–7719. [PubMed: 16120771]
7. Kapogiannis D, Mattson M. Disrupted energy metabolism and neuronal circuit dysfunction in cognitive impairment and Alzheimer's disease. *Lancet Neurol*. 2011; 10:187–198. [PubMed: 21147038]
8. Buckner R, Sepulcre J, Talukdar T, Krienen F, Liu H, Hedden T, et al. Cortical hubs revealed by intrinsic functional connectivity: mapping, assessment of stability, and relation to Alzheimer's disease. *J Neurosci*. 2009; 29:1860–1873. [PubMed: 19211893]
9. Oh H, Mormino E, Madison C, Hayenga A, Smiljic A, Jagust W. β -Amyloid affects frontal and posterior brain networks in normal aging. *Neuroimage*. 2011; 54:1887–1895. [PubMed: 20965254]
10. Rentz D, Locascio J, Becker J, Moran E, Eng E, Buckner R, et al. Cognition, reserve, and amyloid deposition in normal aging. *Ann Neurol*. 2010; 67:353–364. [PubMed: 20373347]
11. Dosenbach N, Nardos B, Cohen A, Fair D, Power J, Church J, et al. Prediction of individual brain maturity using fMRI. *Science*. 2010; 329:1358–1361. [PubMed: 20829489]
12. van den Heuvel M, Stam C, Boersma M, Hulshoff Pol H. Small-world and scale-free organization of voxel-based resting-state functional connectivity in the human brain. *Neuroimage*. 2008; 43:528–539. [PubMed: 18786642]
13. Beu M, Baudrexel S, Hautzel H, Antke C, Mueller H-W. Neural traffic as voxel-based measure of cerebral functional connectivity in fMRI. *J Neurosci Methods*. 2009; 176:263–269. [PubMed: 18834906]
14. van den Heuvel M, Mandl R, Kahn R, Hulshoff Pol H. Functionally linked resting-state networks reflect the underlying structural connectivity architecture of the human brain. *Hum Brain Mapp*. 2009; 30:3127–3141. [PubMed: 19235882]
15. van den Heuvel M, Stam C, Kahn R, Hulshoff Pol H. Efficiency of functional brain networks and intellectual performance. *J Neurosci*. 2009; 29:7619–7624. [PubMed: 19515930]
16. Tomasi D, Volkow N. Functional Connectivity Density Mapping. *Proc Natl Acad Sci U S A*. 2010; 107:9885–9890. [PubMed: 20457896]
17. Tomasi D, Volkow N. Association between Functional Connectivity Hubs and Brain Networks. *Cereb Cortex*. 2011 [Epub ahead of print].
18. Buckner R. Human functional connectivity: new tools, unresolved questions. *Proc Natl Acad Sci U S A*. 2010; 107:10769–10770. [PubMed: 20547869]
19. Biswal B, Mennes M, Zuo X, Gohel S, Kelly C, Smith S, et al. Toward discovery science of human brain function. *Proc Natl Acad Sci U S A*. 2010; 107:4734–4739. [PubMed: 20176931]

20. Foerster B, Tomasi D, Caparelli E. Magnetic field shift due to mechanical vibration in functional magnetic resonance imaging. *Magn Reson Med*. 2005; 54:1261–1267. [PubMed: 16215962]
21. Cordes D, Haughton V, Arfanakis K, Carew J, Turski P, Moritz C, et al. Frequencies Contributing to Functional Connectivity in the Cerebral Cortex in “Resting-state” Data. *AJNR Am J Neuroradiol*. 2001; 22:1326–1333. [PubMed: 11498421]
22. Tomasi D, Volkow N. Functional connectivity hubs in the human brain. *Neuroimage*. 2011;10.1016/j.neuroimage.2011.05.024
23. Worsley K, Evans A, Marrett S, Neelin P. A three-dimensional statistical analysis for CBF activation studies in human brain. *J Cereb Blood Flow Metab*. 1992; 12:900–918. [PubMed: 1400644]
24. Fjell A, Walhovd K. Structural brain changes in aging: courses, causes and cognitive consequences. *Rev Neurosci*. 2010; 21:187–221. [PubMed: 20879692]
25. Volkow N, Logan J, Fowler J, Wang G, Gur R, Wong C, et al. Association between age-related decline in brain dopamine activity and impairment in frontal and cingulate metabolism. *Am J Psychiatry*. 2000; 157:75–80. [PubMed: 10618016]
26. Salzman, K., editor. *Clinical Geriatric Psychopharmacology*. Lippincott Williams & Wilkins; Pennsylvania: 2005.
27. Madden D, Bennett I, Song A. Cerebral white matter integrity and cognitive aging: contributions from diffusion tensor imaging. *Neuropsychol Rev*. 2009; 19:415–435. [PubMed: 19705281]
28. Stern Y, Moeller J, Anderson K, Lubner B, Zubin N, DiMauro A, et al. Different brain networks mediate task performance in normal aging and AD: defining compensation. *Neurology*. 2000; 55:1291–1297. [PubMed: 11087770]
29. Reuter-Lorenz P, Park D. Human neuroscience and the aging mind: a new look at old problems. *J Gerontol B Psychol Sci Soc Sci*. 2010; 65:405–415. [PubMed: 20478901]
30. Craik, F.; Salthouse, T., editors. *The Handbook of Aging and Cognition*. Lawrence Erlbaum Associates, Inc; Mahwah, NJ: 2000.
31. Wingfield A, Grossman M. Language and the aging brain: patterns of neural compensation revealed by functional brain imaging. *J Neurophysiol*. 2006; 96:2830–2839. [PubMed: 17110737]
32. Sanfey, A.; Hastie, R. *Cognitive Aging: A Primer*. Park, D.; Schwarz, N., editors. Psychology Press; Philadelphia, PA: 2000. p. 253
33. Raichle ME, Gusnard DA. Appraising the brain’s energy budget. *Proc Nat Acad Sci USA*. 2002; 99:10237–10239. [PubMed: 12149485]
34. Langbaum J, Chen K, Lee W, Reschke C, Bandy D, Fleisher A, et al. Alzheimer’s Disease Neuroimaging Initiative. *Neuroimage*. 2009; 45:1107–1116. [PubMed: 19349228]
35. Raichle ME, MacLeod AM, Snyder AZ, Powers WJ, Gusnard DA. A default mode of brain function. *Proc Natl Acad Sci USA*. 2001; 98:676–682. [PubMed: 11209064]
36. Tomasi D, Ernst T, Caparelli E, Chang L. Common deactivation patterns during working memory and visual attention tasks: An intra-subject fMRI study at 4 Tesla. *Hum Brain Mapp*. 2006; 27:694–705. [PubMed: 16404736]
37. Changeux, J. *Neuronal man*. Princeton University Press; New Jersey: 1997.
38. Tootell R, Hadjikhani N, Vanduffel W, Liu A, Mendola J, Sereno M, et al. Functional analysis of primary visual cortex (V1) in humans. *Proc Natl Acad Sci USA*. 1998; 95:811–817. [PubMed: 9448245]
39. Damoiseaux J, Beckmann C, Arigita E, Barkhof F, Scheltens P, Stam C, et al. Reduced resting-state brain activity in the “default network” in normal aging. *Cereb Cortex*. 2008; 18:1856–1864. [PubMed: 18063564]
40. Reyngoudt H, Claeys T, Vlerick L, Verleden S, Acou M, Deblaere K, et al. Age-related differences in metabolites in the posterior cingulate cortex and hippocampus of normal ageing brain: A (1)H-MRS study. *Eur J Radiol*. 2011 [Epub ahead of print].
41. Andrews-Hanna J, Snyder A, Vincent J, Lustig C, Head D, Raichle M, et al. Disruption of large-scale brain systems in advanced aging. *Neuron*. 2007; 56:924–935. [PubMed: 18054866]

42. Sambataro F, Murty V, Callicott J, Tan H, Das S, Weinberger D, et al. Age-related alterations in default mode network: impact on working memory performance. *Neurobiol Aging*. 2010; 31:839–852. [PubMed: 18674847]
43. Kalpouzos G, Chételat G, Baron J, Landeau B, Mevel K, Godeau C, et al. Voxel-based mapping of brain gray matter volume and glucose metabolism profiles in normal aging. *Neurobiol Aging*. 2009; 30:112–124. [PubMed: 17630048]
44. Pardo J, Lee J, Sheikh S, Surerus-Johnson C, Shah H, Munch K, et al. Where the brain grows old: decline in anterior cingulate and medial prefrontal function with normal aging. *Neuroimage*. 2007; 35:1231–1237. [PubMed: 17321756]
45. Filley C, Cullum C. Attention and vigilance functions in normal aging. *Appl Neuropsychol*. 1994; 1:29–32. [PubMed: 16318558]
46. Volkow N, Gur R, Wang G, Fowler J, Moberg P, Ding Y, et al. Association between decline in brain dopamine activity with age and cognitive and motor impairment in healthy individuals. *Am J Psychiatry*. 1998; 155:344–349. [PubMed: 9501743]
47. Tomasi D, Volkow N, Wang G, Wang R, Telang F, Caparelli E, et al. Methylphenidate enhances brain activation and deactivation responses to visual attention and working memory tasks in healthy controls. *Neuroimage*. 2011; 54:3101–3110. [PubMed: 21029780]
48. Schneider-Garces N, Gordon B, Brumback-Peltz C, Shin E, Lee Y, Sutton B, et al. Span, CRUNCH, and beyond: working memory capacity and the aging brain. *J Cogn Neurosci*. 2010; 22:655–669. [PubMed: 19320550]
49. Beason-Held L, Kraut M, Resnick S. I: Longitudinal changes in aging brain function. *Neurobiol Aging*. 2008; 29:483–496. [PubMed: 17184881]
50. Blackstone C, O’Kane C, Reid E. Hereditary spastic paraplegias: membrane traffic and the motor pathway. *Nat Rev Neurosci*. 2011; 12:31–42. [PubMed: 21139634]
51. Calhoun M, Mao Y, Roberts J, Rapp P. Reduction in hippocampal cholinergic innervation is unrelated to recognition memory impairment in aged rhesus monkeys. *Comp Neurol*. 2004; 475:238–246.
52. Marner L, Nyengaard J, Tang Y, Pakkenberg B. Marked loss of myelinated nerve fibers in the human brain with age. *J Comp Neurol*. 2003; 462:144–152. [PubMed: 12794739]
53. Gong G, Rosa-Neto P, Carbonell F, Chen Z, He Y, Evans A. Age- and gender-related differences in the cortical anatomical network. *J Neurosci*. 2009; 29:15684–15693. [PubMed: 20016083]
54. Gur R, Gur R, Obrist W, Hungerbuhler J, Younkin D, Rosen A, et al. Sex and handedness differences in cerebral blood flow during rest and cognitive activity. *Science*. 1982; 217:659–661. [PubMed: 7089587]
55. Baxter LJ, Mazziotta J, Phelps M, Selin C, Guze B, Fairbanks L. Cerebral glucose metabolic rates in normal human females versus normal males. *Psychiatry Res*. 1987; 21:237–245. [PubMed: 3498176]
56. Pernecky R, Drzezga A, Diehl-Schmid J, Li Y, Kurz A. Gender differences in brain reserve: an (18)F-FDG PET study in Alzheimer’s disease. *J Neurol*. 2007; 254:1395–1400. [PubMed: 17934882]

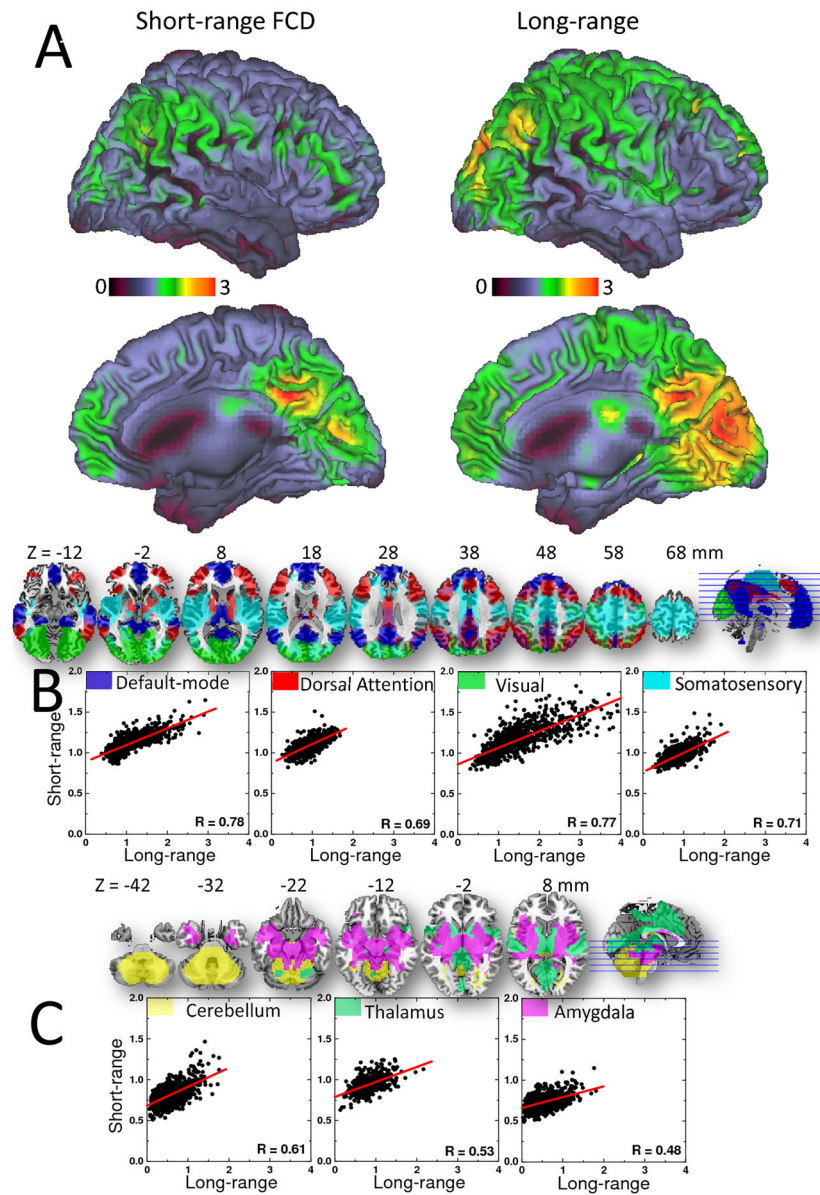


Fig 1.
 Fig 1A: Surface rendering showing the distribution of short- and long-range FCD hubs in the human brain. Color maps reflect the average number of functional connections to neighbor (short-range) or remote (long-range) voxels across 913 healthy subjects. Threshold used to compute short- and long-range FCD: $R > 0.6$. The images were created using the Computerized Anatomical Reconstruction and Editing Toolkit (CARET) 5.0 (<http://brainvis.wustl.edu/wiki/index.php/Caret>About>). **B:** Scatter plots depicting the linear association between short- and long-range FCD in four cortical networks (axial views). **C:** Scatter plots depicting the linear association between short- and long-range FCD in three subcortical networks (axial views).

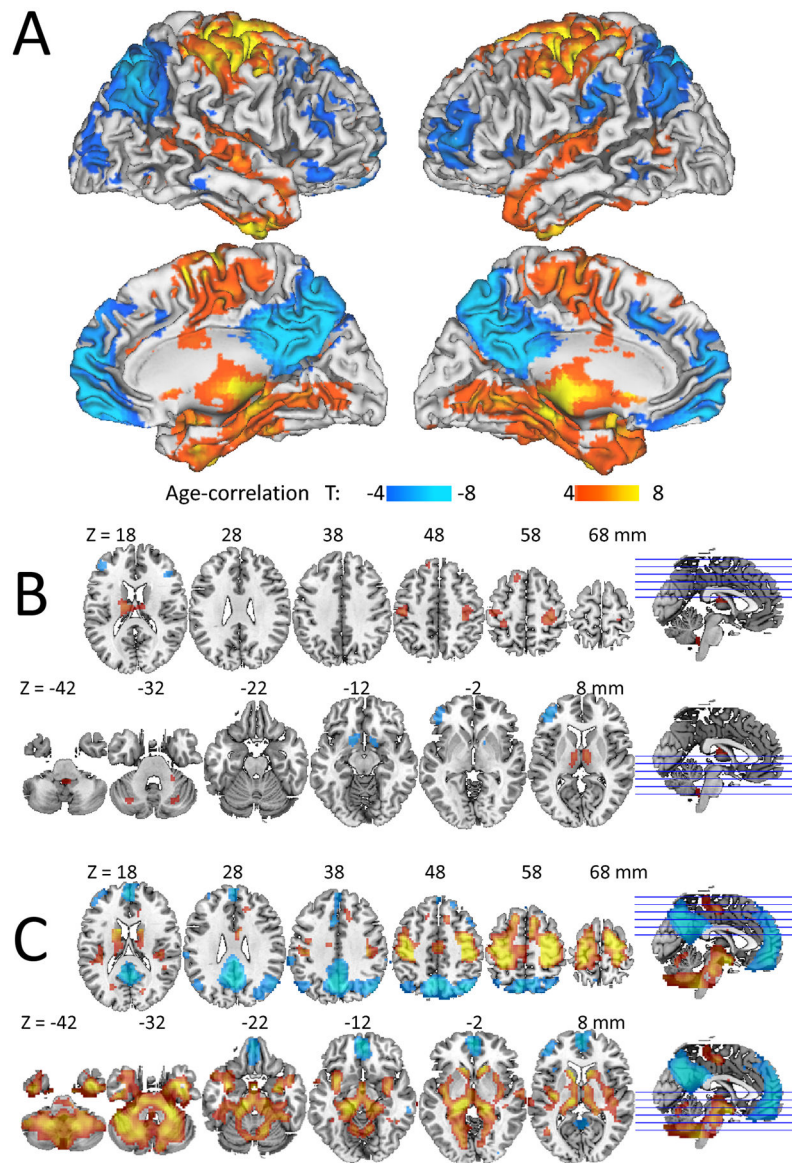


Fig 2.

Fig 2A: Statistical significance (T-score) of the correlation between long-range FCD and age across 913 healthy subjects, overlaid on the surface of the Colin template. Statistical significance of correlations with age for **B**: short-range and **C**: long-range FCD superimposed on MRI axial views of the human brain.

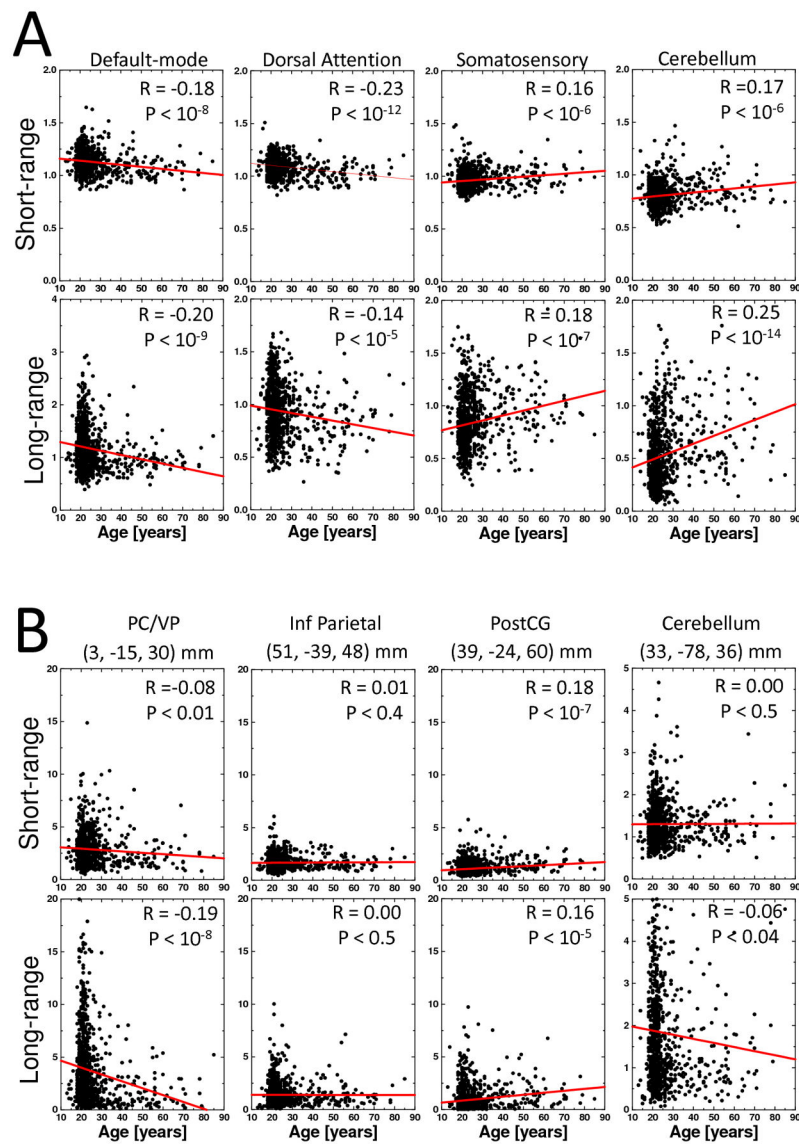


Fig 3. Scatter plots showing age-related changes in short- and long-range FCD. Average FCD values across voxels in cortical and subcortical networks (**A**) and at the location of major cortical and subcortical hubs (**B**). Lines are linear fits of the data. Sample: 913 subjects.

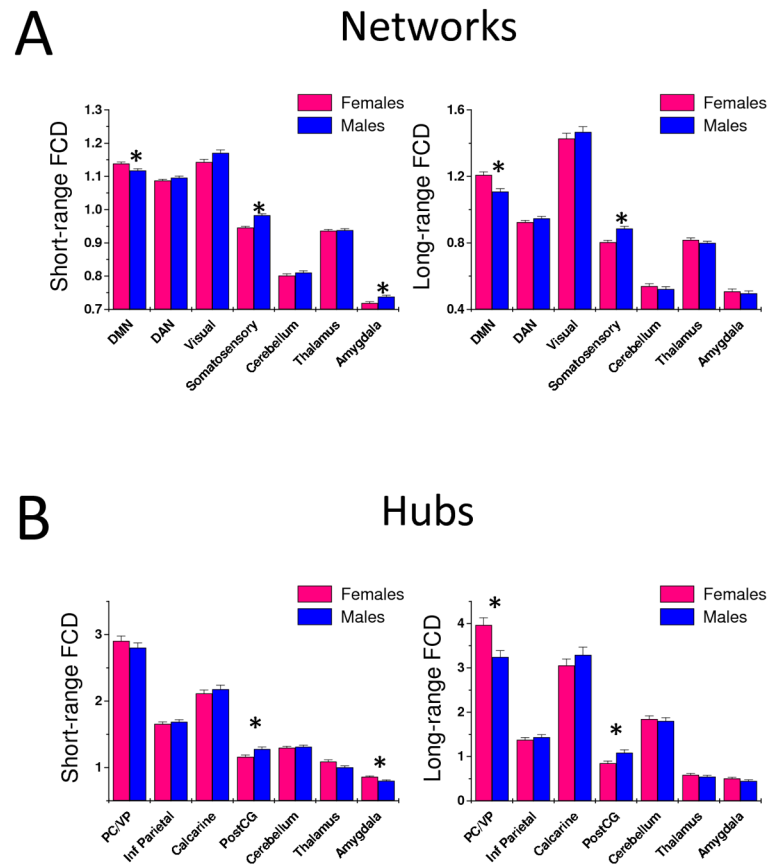


Fig 4. Average values for short- (left) and long-range (right) FCD across subjects and voxels in seven major networks (**A**) and hubs (**B**) for males (N = 408) and females (N = 505). Error bars are standard errors of the mean. (*) Statistical significance for gender differences: P < 0.005.

Short (SR) and long-range (LR) FCD and their correlations with age. Statistical values averaged in 3-mm isotropic (cubic) regions of interest centered at the MNI-coordinates (X, Y, Z) of the local maxima (Fig 2). Sample: 913 healthy subjects.

Table 1

Region	BA	X [mm]	Y [mm]	Z [mm]	SR [T]	LR [T]	SR-age [T]	LR-age [T]	LR-age > SR-age [T]
Precuneus	7	3	-63	36	27.2	47.3	NS	-9.2	-5.6
Precuneus	23	-3	-57	24	27.6	41.6	NS	-8.4	-4.4
Posterior Cingulate	23	-3	-39	27	43.3	43.4	-2.5	-7.7	-3.7
Inferior Parietal	7	-36	-69	48	33	46.1	NS	-7.0	-3.9
Middle Orbital Frontal	11	0	54	-9	26.1	41.5	NS	-8.3	-4.6
Sup Medial Frontal	32	0	54	18	31.5	42.6	NS	-7.0	-3.6
Sup Medial Frontal	9	0	51	42	26.2	30.9	NS	-3.8	NS
Anterior Cingulate	32	6	18	39	53.0	42.1	-2.5	-4.8	NS
MiddleFrontal	45	45	45	6	50.5	31.6	-5.4	-4.9	NS
Supramarginal	40	63	-33	36	37.7	39.1	NS	-5.0	-3.2
Angular	39	48	-66	30	37.7	40.8	NS	-4.6	-2.9
Superior Frontal	9	-21	36	51	25.5	29.1	NS	-3.2	NS
Middle Frontal	9	-42	18	51	28.3	29.2	NS	-3.0	NS
Precentral	44	-48	12	33	54.6	41.4	NS	-2.8	NS
Inferior Frontal	47	36	30	3	53.8	32.3	-3.2	NS	NS
Middle Frontal	46	33	45	24	50.0	35.0	-3.1	-3.5	NS
Nucleus accumbens	25	15	12	-12	58.4	27.2	-5.0	NS	3.2
Nucleus accumbens	25	-12	9	-9	59.2	28.9	-4.6	NS	3.5
Rectus	11	0	21	-24	20.6	23.4	-3.1	-3.5	NS
Inferior Frontal	45	-42	30	18	56.4	32.9	-4.1	-3.2	NS
Caudate	9	15	6	6	31.7	12.6	NS	4.8	3.3
Postcentral	4	-24	-30	63	41.9	27.5	5.5	10.6	3.7
Precentral	6	-24	-15	63	47.8	29.5	3.0	10.7	5.4
Postcentral	3	42	-21	51	41.8	30.1	4.8	9.1	3.0
Thalamus	12	-24	-24	3	50.8	24.2	3.6	9.2	3.9
Hippocampus	27	21	-30	-6	45.7	28.8	3.6	9.1	3.9

Region	BA	X [mm]	Y [mm]	Z [mm]	SR [T]	LR [T]	SR-age [T]	LR-age [T]	LR-age > SR-age [T]
Fusiform	37	-24	-36	-33	54.7	25.8	3.2	8.9	4.0
Hippocampus	27	-18	-30	-3	57.0	28.1	NS	7.7	4.1
Fusiform	36	-36	0	-39	50.8	22.1	NS	8.3	4.8
Insula	13	36	-15	6	46.9	29.0	NS	6.9	3.9
Cerebellum	36	36	-3	-27	29.7	19.1	NS	4.7	3.1
Pons	12	12	-27	-24	24.6	26.0	NS	8.7	4.7
Heschl	13	-42	-24	12	42.9	36.2	NS	5.3	2.8
Superior Temporal	22	-63	-15	0	35.9	39.0	NS	5.2	3.1
Middle Cingulate	24	-9	3	30	27.5	19.6	NS	3.1	NS
Middle Temporal	21	-45	-45	15	33.0	21.6	NS	2.9	NS
Superior Temporal	41	39	-33	15	40.1	29.9	NS	4.9	2.5
Fusiform	37	39	-48	-18	45.2	33.9	NS	4.5	NS
Middle Cingulate	23	12	-12	36	45.9	24.5	NS	3.7	2.7
Inferior Temporal	20	42	-21	-24	34.6	18.0	NS	3.6	NS
Superior Temporal	22	69	-18	6	21.1	23.2	NS	2.9	NS
Calcarine	18	-18	-75	18	32.9	39.2	NS	3.6	NS